Biol Cybern (2007) 96:407–419
DOI 10.1007/s00422-006-0139-8

ORIGINAL PAPER

Biological Cybernetics

Neuronal firing rates account for distractor effects on mnemonic accuracy in a visuo-spatial working memory task

Julian Macoveanu · Torkel Klingberg · Jesper Tegnér

Received: 3 June 2005 / Accepted: 2 November 2006 / Published online: 27 January 2007

Abstract Persistent neural activity constitutes one neuronal correlate of working memory, the ability to hold and manipulate information across time, a prerequisite for cognition. Yet, the underlying neuronal mechanisms are still elusive. Here, we design a visuo-spatial delayed-response task to identify the relationship between the cue-distractor spatial distance and mnemonic accuracy. Using a shared experimental and computational test protocol, we probe human subjects in computer experiments, and subsequently we evaluate different neural mechanisms underlying persistent activity using an in silico prefrontal network model. Five modes of action of the network were tested: weak or strong synaptic interactions, wide synaptic arborization, cellular bistability and reduced synaptic NMDA component. The five neural mechanisms and the human behavioral data, all exhibited a significant deterioration of the mnemonic accuracy with decreased spatial distance between the distractor and the cue. A subsequent computational analysis revealed that the firing rate and not the neural mechanism per se, accounted for the positive correlation between mnemonic accuracy and spatial distance. Moreover, the computational modeling predicts an inverse correlation between accuracy and distractibility. In conclusion, any pharmacological modulation, pathological condition or memory training paradigm targeting the underlying neural circuitry and altering the net population firing rate during the delay is predicted to determine the amount of influence of a visual distraction.

J. Macoveanu · J. Tegnér
Computational Biology, Department of Physics,
Linköping University of Technology,
581 83 Linköping, Sweden

T. Klingberg
Department of Woman and Child Health, MR center,
Karolinska Institutet, 171 76 Stockholm, Sweden

J. Tegnér
Computational Medicine Group, Department of Medicine,
Karolinska Institutet, 171 76 Stockholm, Sweden

J. Tegnér (✉)
Division for Computational Biology,
Department of Physics, IFM,
Linköping University of Technology,
581 83 Linköping, Sweden
e-mail: jespert@ifm.liu.se

1 Introduction

Working memory (WM), the capacity to hold and manipulate information during a brief period of time, is central for cognitive performance including language, problem solving and it also constitutes a basis for guiding future actions (Norman 1970; Baddeley 1986). The transient storage governed by WM is an active and dynamic process, where persistent and stimulus selective elevated neural activity has been identified as one neural correlate for visuo-spatial WM (Goldman-Rakic 1995; Wang 2001). Posterior parietal, inferotemporal and prefrontal cortical areas are closely associated with WM, as demonstrated by lesion, brain imaging and electrophysiological studies (Goldman-Rakic 1987, 1995; Fuster 1995). If the persistent activity is disrupted by electrical stimulation or by distracting stimuli during the delay period, the cue-related information in memory is lost (Funahashi et al. 1989; Fuster 1997). Consequently, neural control of the sustained delay activity and robustness against distractors is crucial for an intact cognitive apparatus.

Yet, the underlying neuronal mechanisms which govern the sustained activity and control the sensitivity against distractors have not yet been identified. Computational modeling of cortical circuits is an important research tool which facilitates an identification of the contribution from different synaptic and cellular factors (Wang 2001). Here, we use a biophysical network model operating in different modes to produce persistent activity where our objective is to evaluate different cellular and synaptic mechanisms which have been suggested to generate persistent neuronal activity in connection with a visuo-spatial WM tasks. We used spatially distracting stimuli to investigate both the different regimes of the network model and behavioral experiments performed on human subjects. Specifically, we investigated the relationship between spatial distance to distractors and mnemonic accuracy in a visuo-spatial delayed-response task. Our integrated experimental and computational distractor design enables us to correlate the spatial sensitivity between distractors and mnemonic accuracy for different neural mechanisms with human behavior.

For cortical networks in general, several broad classes of neural mechanisms have been discussed. First, synfire chains—chains of neuronal subgroups feedforward connected—that permit a wave of synchronous activity to be maintained through closed loops (Abeles 1991; Diesmann et al. 1999; Gewaltig et al. 2001); synchronous oscillations as a basis for cortical dynamics subserving perception, memory and cognition (Singer 1993); networks operating with fast Hebbian plasticity (Brunel 1996; Sandberg et al. 2003). However, the most accepted and biologically plausible mechanistic framework in the field of visuo-spatial or object working memory is a recurrent network model in which the persistent activity is represented as self-sustained dynamically stable states through reverberatory neural activity (Amari 1977; Hopfield 1982; Amit 1995). This mechanism was first investigated in the 1930s by Lorente de Nó and Hebb (1949) and refers to the flow of neural activity due to the early observation that cerebral cortex has an abundance of recurrent synaptic connections between neurons. Several studies concerning the neural mechanisms underlying WM activity have been performed using different neuronal and synaptic instances of this basic recurrent neural network idea originating from the work of Lorente de Nó and Hebb (Seung 1996; Amit and Brunel 1997; Fransen and Lansner 1998; Compte et al. 2000; Seung et al. 2000; Tegnér et al. 2002; Egorov et al. 2002; Koulakov et al. 2002; Goldman et al. 2003; Loewenstein and Sompolinsky 2003; Wang et al. 2004). These computational studies have revealed that even though the mechanistic framework based on the reverberatory idea appears straightforward, there are several non-trivial issues such as what controls the firing rate and the stability of the neural activity during the delay-period. Thus, the major reason why there are several different versions of the original reverberatory circuit is that those issues depend on the particular nature of the neuronal and synaptic mechanisms governing the persistent activity. Our strategy here is to evaluate the major modes of operations by investigating the consequences of a distractor in the different neural modes of action for the network. The advantage is that the outcome of those in silico experiments can be directly evaluated using the human behavioral experiments we have performed in the present study.

Due to the inherent stability problems with the recurrent model several modifications have been suggested such as an increased synaptic NMDA component and stronger or wider excitatory synaptic connections (Amit and Brunel 1997; Compte et al. 2000; Tegnér et al. 2002). Additionally, as it recently gained more experimental support (Egorov et al. 2002), cellular bistability has been suggested to stabilize the persistent activity (Koulakov et al. 2002). A bistable mode of action allows neurons to jump between two stable activity states with low and high firing rates. Goldman et al. (2003) reduced the large jumps in firing rates commonly associated with bistability by incorporating multiple dendritic subunits. As a consequence, the firing rate of a neuron increases only incrementally as single dendritic compartments switch state. To evaluate these different mechanistic proposals, we first implemented the biophysical network model in a reference mode (A) from which we can modify the model parameters to enable the following different modes of action: strong recurrent excitatory synaptic connections, referred to as (B) high E-E mode; wider excitatory connections, referred to as (C) wide profile mode; a bistable mode of action, referred to as (D) bistable mode; and finally a low NMDA synaptic component, referred to as (E) low NMDA mode.

2 Methods

2.1 Behavioral distractor trial

A visuo-spatial WM task using visual distractors during the delay period was performed by 31 participants (14 men and 17 women, average age 25.8 ± 4.6). They were asked to remember the spatial position of five blue circles (cues) which appeared one at a time on a 28.5×21.5 cm computer monitor, 50 cm distance from the participant's eyes. The cues and distractors could appear at 16 possible locations on the perimeter of a

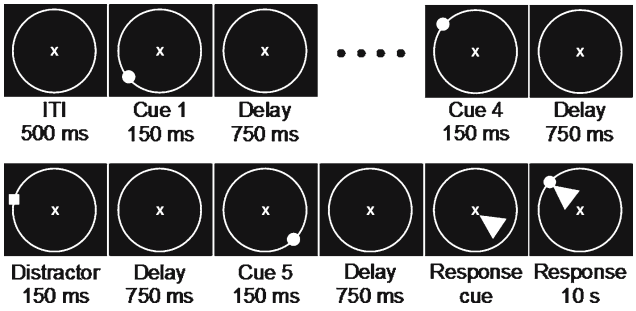

Fig. 1 Schematic diagram showing an example of the delayed-response task. The participants fixed their gaze on a central spot during the entire task. After a fixation screen of 500 ms five cues (*circles*) and one distractor (*square*) were presented at different locations on the peripheral circle with 150 ms presentation time and 750 ms inter-cue delay. Distractors followed the third or the fourth cue at five distances, 22.5°, 45°, 67.5°, 90° and 180°. After the cue presentation the participants indicated in an orderly manner the location of each cue with the computer mouse

circle of 20.0 cm diameter which was visible during the entire task (Fig. 1).

The participants initiated the trial fixating a point for 500 ms in the center of the screen and were asked to maintain fixation during the entire trial. The fixation period was followed by a succession of five cues (blue circles) and one intervening distractor (blue square), with 150 ms presentation time and 750 ms delay between the cues. The last cue was followed by a delay period of 750 ms after which the cursor of a computer mouse appeared and the participants had to respond by clicking on the remembered cue locations.

In every trial either the third or the fourth cue was followed by a distractor that was to be ignored. The distractor could be presented at five spatial distances relative to the memorized cue, 22.5°, 45°, 67.5°, 90° and 180° angles with the vertex on the fixation point. Thus, 360° represented the whole span of the visual field. The shorter the distance the higher was the expected interference of the distractor with the memory of the cue. A total of 40 trials were performed in random order by every participant.

The distractor effect was evaluated by means of accuracy, defined as the spatial distance (measured in degrees) from the presented cue to the location indicated by the participant at the end of the trial (~4 s after cue onset).

The participants responded by clicking on the screen (continuous range of locations) for all five memorized cues in the order of appearance. If the distance from the cue location to the location pointed out by the participant (accuracy) exceeded a predefined threshold of 20° the cue location was considered forgotten and the trial was discarded. Only the accuracy of the cue followed by distractor and its corresponding control (no distraction) were taken into consideration.

The significance of the behavioral results was assessed using one-way repeated-measure ANOVA and two-sided paired *t*-test.

2.2 Recurrent network model

The neural network model used for the simulations was previously studied by Tegnér et al. (2002) and represents a local cortical circuit capable of upholding states of persistent neuronal activity accounting for the memory storage in WM (Amit and Brunel 1997; Wang 1999; Compte et al. 2000; Tegnér et al. 2002). The model included 2 neuronal populations, 512 excitatory (E) and 128 inhibitory (I) cells (Fig. 2a). The neurons were spatially distributed in a ring in accordance with the preferred visual angle of the stimulus location. Thus, the neurons responded selectively to visual stimuli depending on their spatial location in the visual field (Ben-Yishai et al. 1995), resembling previous oculomotor delayed-response task experiments (Funahashi et al. 1989; Goldman-Rakic 1995). The neurons were parameterized by the angle θ (0°–360°) that specified their preferred visual angle. Figure 2b shows a schematic diagram of the connectivity structure. The architecture of the model and its recurrent connectivity resembles the columnar organization of the prefrontal cortex (Levitt et al. 1993; Goldman-Rakic 1995; Kritzer and Goldman-Rakic 1995; Mountcastle 1997). The neuron models used followed the Hodgkin–Huxley formalism with action potential profile and neuronal input–output relation calibrated using cortical-slice data (McCormick et al. 1985; Markram et al. 1997) and the postsynaptic current gating kinetics of AMPA, NMDA (Hestrin et al. 1990; Jahr and Stevens 1990; Spruston et al. 1995) and $GABA_A$ receptors (Amari 1977; Salin and Prince 1996; Xiang et al. 2002).

Excitatory neurons were of pyramidal type with three compartments, representing soma, proximal and distal dendrites. The somatic compartment contains I_{Na} and I_K currents, a high-threshold calcium current I_{Ca}, and a slow calcium-dependent cationic current I_{CAN}. The proximal dendritic compartment has a persistent sodium current I_{NaP} and a slowly inactivating potassium current I_{KS}. The distal dendritic compartment has an I_{Ca} and a transient A-type potassium current I_A. Additionally, all neuronal compartments included a leak current I_L. The membrane equations for the somatic voltage V_s, proximal dendritic voltage V_{d1}, and distal dendritic voltage V_{d2} were

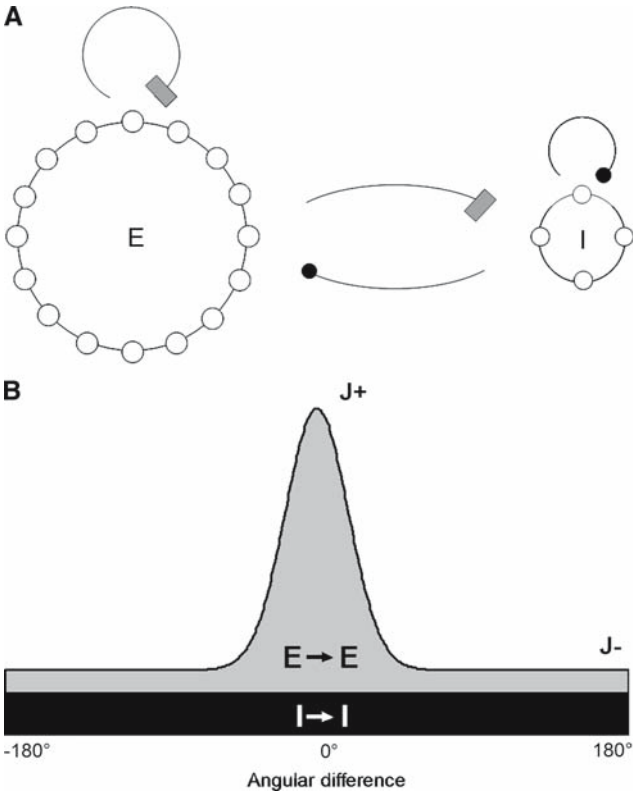

Fig. 2 Schematic representation of the model connectivity. **a** Two populations of neurons 512 excitatory (E) and 128 Inhibitory (I) cells with all-to-all connections both within and between the populations. **b** The strength of the recurrent connections between excitatory cells depended on their proximity, represented by the angle between them. Inhibitory projections, which extend to all cells, are evenly distributed across the pyramidal and inhibitory units of the network. See text for more details

$$\frac{C_m \mathrm{d}V_s}{\mathrm{d}t} = -I_{\mathrm{Na}} - I_{\mathrm{K}} - I_{\mathrm{Ca}} - I_{\mathrm{L}} - I_{\mathrm{CAN}} - \frac{gc_1(V_s - V_{\mathrm{d1}})}{p_1 - I_{\mathrm{syn}}}$$

$$\frac{C_m \mathrm{d}V_{\mathrm{d1}}}{\mathrm{d}t} = -I_{\mathrm{NaP}} - I_{\mathrm{KS}} - I_{\mathrm{L}} - \frac{gc_1(V_{\mathrm{d1}} - V_s)}{p_2} - \frac{gc_2(V_{\mathrm{d1}} - V_{\mathrm{d2}})}{p_2 - I_{\mathrm{syn}}}$$

$$\frac{C_m \mathrm{d}V_{\mathrm{d2}}}{\mathrm{d}t} = -I_{\mathrm{A}} - I_{\mathrm{Ca}} - I_{\mathrm{L}} - \frac{gc_2(V_{\mathrm{d2}} - V_{\mathrm{d1}})}{(1 - p_1 - p_2) - I_{\mathrm{syn}}}.$$

The inhibitory neurons were of fast-spiking type and were represented by one compartment containing only spike generating sodium and potassium currents. The membrane equation was

$$\frac{C_m \mathrm{d}V}{\mathrm{d}t} = -I_{\mathrm{Na}} - I_{\mathrm{K}} - I_{\mathrm{Ca}} - I_{\mathrm{L}}.$$

Synaptic currents were modeled according to $I_{\mathrm{syn}} = g_{\mathrm{syn}} s(V - E_{\mathrm{syn}})$, where g_{syn} represents the maximal synaptic conductance, E_{syn} the synaptic reversal potential and s is the gating variable which decides the fraction of open synaptic ion channels. A complete description of neuron models, with details of ion channel kinetics and conductance parameters, can be found in (Tegnér et al. 2002).

The synaptic connection strength between excitatory E neurons decreases with the angle between the preferred cues of two neurons following a smooth Gaussian connectivity drop-off. The connectivity W between neuron i and j is described by (Compte et al. 2000)

$$W(\theta_i - \theta_j) = J^+ + (J^- - J^+)\mathrm{e}^{-(\theta_i - \theta_j)^2/2\sigma^2}.$$

$W(\theta_i - \theta_j)$ is the normalized connectivity. The J^- parameter represents the strength of the weak distant connections, J^+ the strength of the stronger adjacent connections and σ the footprint of the connectivity. The excitatory connection strength from E to I as well as all inhibitory connection from I neurons is independent on the inter-neuronal distance and is evenly distributed across the E and I units of the network. The recurrent excitatory synaptic conductances of the model were mediated by NMDA and AMPA receptor channels. Previous theoretical studies (Amari 1977; Lisman et al. 1998; Wang 1999; Compte et al. 2000; Tegnér et al. 2002) revealed that a dominant slow excitation mediated by NMDA receptors stabilizes the firing rate of the pyramidal neurons generating the sustained activity.

2.2.1 Reference parameters

Conductances (mS/cm^2). NMDA channels: $g_{\mathrm{EE}} = 1.67$, $g_{\mathrm{EI}} = 1.19$; AMPA channels: $g_{\mathrm{EE}} = 0, g_{\mathrm{EI}} = 0$; GABA receptors: $g_{\mathrm{IE}} = 1.29, g_{\mathrm{II}} = 0.65$.

Connectivity. $\mathrm{J}^+ = 5.25, \sigma = 0.05$.

Overall external excitation: uncorrelated Poisson spike trains of 1,000 Hz per cell mediated by AMPA receptors; conductances (mS/cm^2): $g_{\mathrm{ext,E}} = 0.235, g_{\mathrm{ext,I}} = 0.042$.

2.2.2 Modeled neural mechanisms

We studied five distinct network instances, all based on excitatory reverberation, but with potentially alternative neural mechanisms: reference mode (A), high E–E mode (B), wide profile mode (C), bistable mode (D) and low NMDA mode (E). The distinction was assessed by simulations of all network instances using a common simulation protocol with one cue and one distractor.

The reference mode (A), which used the unchanged reference parameters, was characterized by low connectivity between the excitatory cells. The rest of the network modes contained a single modified characteristic

compared to the reference mode. For the high excitatory connectivity mechanism employed in the high E–E mode (B), the peak conductance of the NMDA channels was increased, $g_{EE} = 1.82\,\mathrm{mS/cm^2}$. The wide profile mode (C) used a wide footprint of the excitatory connectivity. This was achieved by simultaneously decreasing the strength of the adjacent E–E connection ($J^+ = 4$) and increasing the connectivity footprint ($\sigma = 0.07$).

The bistable mode (D) used excitatory units with a bistable regime in their firing pattern. Cellular bistability have been attributed to voltage-dependent components that can exhibit self-sustained activation, such as the NMDA channel and voltage-sensitive Ca^{2+} channels (Lee and Heckman 1998; Schiller and Schiller 2001). Our model incorporated a Ca^{2+}-activated non-selective cationic (CAN) current into the membrane of the distal dendritic compartment of the pyramidal cells (Tegnér et al. 2002). This slow calcium-dependent current has been identified in rat prefrontal neurons (Haj-Dahmane and Andrade 1998). The bistable behavior of the neuronal units allows them to switch between a low state and a high state of activity depending on the temporary progress of the current magnitude. The size of the bistable regime is proportional to the magnitude of the I_{CAN} channel conductance (g_{CAN}). We used a g_{CAN} value of $0.2\,\mathrm{mS/cm^2}$ to assure a significant proportion of the active units in the high mode of firing. One observed advantage of networks composed of bistable units is their ability to resist parameter modification to a higher degree. The mechanisms underlying bistability are not thought to influence this attribute (Koulakov et al. 2002). Nonetheless, the biological substrate for bistable neurons in human prefrontal cortex remains elusive.

For the low NMDA mode (E) the excitatory synaptic transmission was dominated by AMPA receptor currents. As previous work suggested, a substantial AMPA component will destabilize the network by the induced synchronous activity of the neurons (Wang 1999; Compte et al. 2000; Gutkin et al. 2001). The NMDA-to-AMPA transmission ratio was gradually reduced while preserving the total synaptic input current until the persistent activity state was lost. For the Low NMDA mode we used a ratio of 30% NMDA receptor current. The conductances of the NMDA and AMPA receptors were calculated using their relative contribution to the time integral of a unitary excitatory postsynaptic current (EPSC) at −65 mV (Compte et al. 2000).

2.2.3 Network simulation protocol

The simulation protocol was chosen to replicate the behavioral distractor trial protocol. However, only the cue with the following distractor have been simulated in the network instances. The models received only background activity the first 500 ms of the simulation. Both cues and distractors were presented as synaptic inputs which lasted for 150 ms and had identical stimulation amplitudes. The cue consisted of a $0.8\,\mu\mathrm{A/cm^2}$ current injected in the distal dendritic compartment which was administrated to a population of 20 pyramidal neurons having the preferred angle between 160° and 180°. The distractor current had identical characteristics as the cue, and was elicited 750 ms after the cue onset at ten different locations on the cell ring, ranging from 22.5° to 180° and including the five locations from the behavioral trial.

3 Results

We studied the relationship between spatial distance to distractors and mnemonic performance in a behavioral WM task. The experimental protocol was used in a computer simulation of sustained activity in the prefrontal cortex. Five distinct neural mechanisms were tested in different modes of a recurrent network model.

3.1 Visuo-spatial WM task

The behavioral results for the 31 participants are presented in Fig. 3. The average accuracies (±SEM) as a function of the distractor distance were $7.4 \pm 3.8°$, $7.2 \pm 2.7°$, $6.8 \pm 2.9°$, $6.6 \pm 2.4°$, $6.5 \pm 3.1°$, for the distractor distances of 22.5°, 45°, 67.5°, 90°, 180°, respectively, and $6.1 \pm 2.6°$ for the undistracted control. A *t*-test for the difference between average accuracies of distractor distances and control was significant only for the closest distractor ($P < 0.05$ for 22.5° and $P > 0.05$ for longer distractor distances). If the individual averages were taken into consideration, a one-way ANOVA testing the dependency on the distractor distance was found significant ($P < 0.05$). The post-test for linear trend between the means for every distance was highly significant ($P < 0.01$, slope −0.55). Furthermore, accuracy slopes calculated for all participants were significantly different form the null hypothesis (*t*-test, $P < 0.05$). The behavioral results suggest that a cue which is similar to a distractor will perturb the remembered target location with the highest effect being achieved with the smallest distractor–target distance.

3.2 Neural network model

3.2.1 Spatiotemporal firing patterns

Figure 4 shows the raster plots for the network model using the reference parameters. All network instances

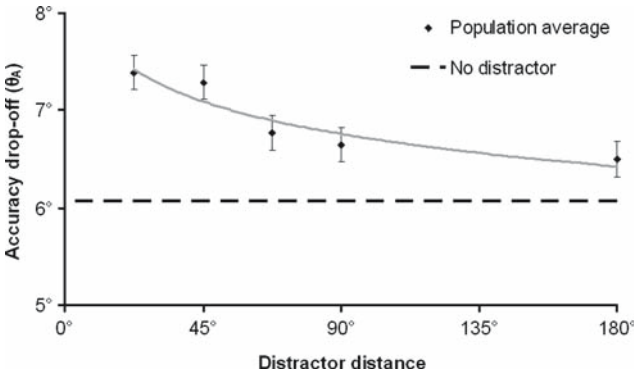

Fig. 3 Behavioral task results. The average accuracy drop-off for all participants as a function of the distractor distance: higher distance leads to better accuracy (lower values). Visual distractors appeared at 22.5°, 45°, 67.5°, 90° and 180°. The control baseline represents average accuracy for undistracted targets. The points are fitted with an exponential decay curve

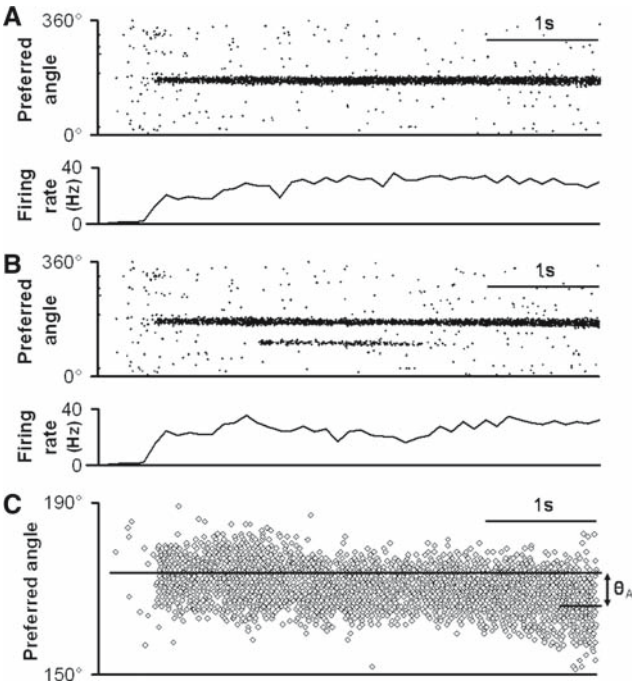

Fig. 4 Spatially localized persistent activity state of the network models. The dots correspond to action potentials from pyramidal cells. The *x* axis represents time, while *y* axis the preferred cue (0°–360°) of the neurons. The cue is presented during 150 ms, to a small fraction of the neurons with a preferred cue at 180°. A persistent activity state is induced by the cue which lasts during the entire delay period. The lower trace represents the average firing rate (100 ms bins) for the bump attractor population. **a** Network simulation of the reference mode. **b** Reference mode with a distractor induced at 56.25° from the memorized cue. **c** Example of accuracy drop-off of the memorized cue calculation for the reference mode with distractor presented at 56° (not shown). The angle θ_A is the average difference between the initial bump location and post-delay location

used the same stimulation protocol as the behavioral distractor trial. The initial state of the network (0–500 ms) was dominated by background activity. A transient cue stimulus of 150 ms triggers the formation of a spatially localized persistent activity state (bump attractor) which was sustained during the whole simulation time (Fig. 4a). The raster plot in Fig. 4b exemplifies a simulation with distractor induced at 56.25° distance. We used the accuracy of the bump state location to quantify the distractor distance effect. The accuracy was calculated as the average difference (θ_A) between the initial cue location right after the cue onset time and the bump state location after a delay period of 4 s (Fig. 4c).

3.2.2 Population firing profile

Electrophysiological studies performed on the prefrontal cortex of monkeys have reported neuronal firing rates of around 20 Hz for the neurons involved in the delay activity of delayed response tasks (Fuster 1973; Funahashi et al. 1989). However, more recent studies have observed firing rates up to more than 60 Hz when the cue is preferred (Constantinidis et al. 2001; Compte et al. 2003). By allowing the slow NMDA currents to dominate the synaptic transmission, cortical network models report firing rates in the range of 20–40 Hz (Compte et al. 2000; Durstewitz et al. 2000).

Figure 5a shows the bump population firing profile averaged over the last 500 ms of the simulation time. The reference mode (A) demonstrated a narrow tuning curve with low firing rates for the bump attractor population (average 22.9 Hz). The high E–E mode (B) approached to the highest degree biophysical data, showing a wide tuning curve, close to physiological shapes found in monkeys (Funahashi et al. 1989) and bump firing rates still within physiological range (average 37.5 Hz). The reduced adjacent E–E connection strength of the wide profile mode (C) resulted in low bump firing rates (average 20.5 Hz). The bistable units of the bistable mode (D) showed as expected elevated firing rates (average 32.1 Hz). The low NMDA mode (E) had a narrow tuning curve with very high firing rates (average 45 Hz). If a distractor is induced in the network the firing rates of the initial bump measured immediately after the distractor onset will be lowered, with the highest effect observed for the closer distractors (Fig. 5b). Resistance to distractor influence proves to be positively correlated with the firing rates across the five network models tested.

3.2.3 Dependence on distractor distance

Figure 6a shows the accuracy of the memorized cue for all five studied neural mechanisms as a function of the

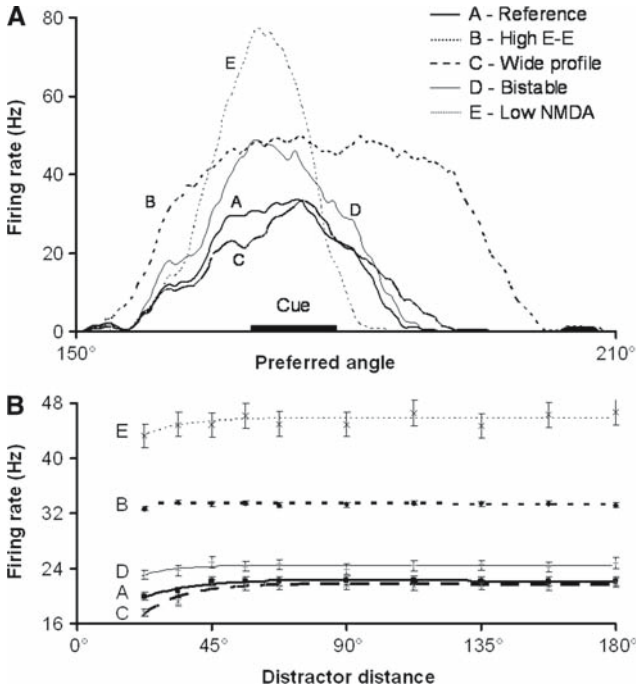

Fig. 5 Firing rate plots. **a** Population firing profile. Average firing rates of the undistracted memory bump for the last 500 ms of the simulation time. All modes except the low NMDA mode generated firing rates within physiological values. Reference mode: average 22.9, peak 36 Hz. High E-E mode: average 37.5, average peak 56 Hz. Wide profile mode: average 20.5, peak 38 Hz. Bistable mode: average 32.1 peak, 52 Hz. Low NMDA mode: average 45.0, peak 78 Hz. (B) Firing rates of the memory bump in a time window of 500 ms directly after distractor onset as function of distractor distance. The points are average of eight noisy simulations and fitted with an exponential decay curve

distractor distance. The modeled mechanism demonstrated to have a clear distractor distance effect, with the highest effect observed at the two closest distractor distances (22.5° and 33.75°). This distance dependency resembles the connectivity curve of the E population (Fig. 2b) which presented a Gaussian drop-off in g_{EE} with the E–E distance. The smooth drop-off in accuracy with distractor distance of the high E–E (B) and low NMDA (E) modes resembled to the highest degree the behavioral results. Differentiating these mechanisms from the mechanisms with low excitatory connectivity, the reference (A), wide profile (C) and bistable (D) modes which showed a similar close distractor effect seems straightforward. However, the similar behavior of the unrelated mechanisms of high E–E (B) and low NMDA (E) modes as well as the dissimilar performance of the closely related reference (A) and high E–E (B) modes indicate that the neural mechanism per se is insufficient to account for the distractor distance effect. We therefore tested whether the difference in the accuracies of the memorized cue is mainly attributed to the firing rate of the bump attractor. For this, we adjusted the inhibitory feedback (g_{IE}) to the excitatory cells in order to alter the firing rates of the five mechanisms and bring them in the smallest range possible. Figure 6b shows accuracy as function of distractor distance for modes A, B, C and D with bump firing rates adjusted to 24.8, 26.5, 26.3 and 23.4 Hz, respectively. The firing rates of the low NMDA (E) mode could not be reduced to values lower than 44.8 Hz, thus this mechanism was ineligible. For the closest distractor distance (22.5°), the four mechanisms fall within an accuracy range of 7.8° when operating at original firing rates (Fig. 6a). This range decreased to 2.9° with the adjusted firing rates. For the longer distractor distances the range was reduced from 3.9 to 1.9°.

The low NMDA mode (E) was surprisingly robust to distractors. We explain this as a consequence of soaring firing rates of the preferred cue neuronal population (average 45 Hz). The drift of the bump is stabilized due to the high level of feedback inhibition that promptly rejects any new incoming stimuli. Given the fast decay of AMPA currents, AMPA synapses remain unsaturated while NMDA receptors saturate during the persistent activity state of the network. For the same input current, AMPA needs to surpass NMDA receptors peak conductance, consequently a dominant AMPA component to the total synaptic drive leads to elevated firing rates.

In a subsequent analysis we mapped the whole feasible range of firing rates for the five neural mechanisms as a function of accuracy. All network modes showed a clear correlation between firing rate and accuracy (Fig. 6c). Although showing the same accuracy—firing rate correlation, the low NMDA (E) mode can be isolated from the rest of the studied mechanisms due to elevated bump firing rates.

These results suggest that the firing rate of the bump attractor is the key factor influencing the accuracy of the memorized cue. However, the firing rate may not be the only factor responsible for the memory drift, but the particular firing pattern given by a neural mechanism may account for some variation as all points in Fig. 6c did not fall on a universal line. The low NMDA (E) mode in particular, which generated highly synchronous activity, showed higher accuracy drop-offs than expected for its bump firing rates.

3.2.4 Mode-dependent parameter range

We mapped the span of the excitatory connection strength mediated by the NMDA receptor channels within the limits imposed in order to preserve the dynamic stability of the network. We gradually increased the peak conductance of NMDA transmission from 1.67 to 1.82 mS/cm^2 (Fig. 7a). All other parameters were unchanged. The lower limit marks the least synaptic

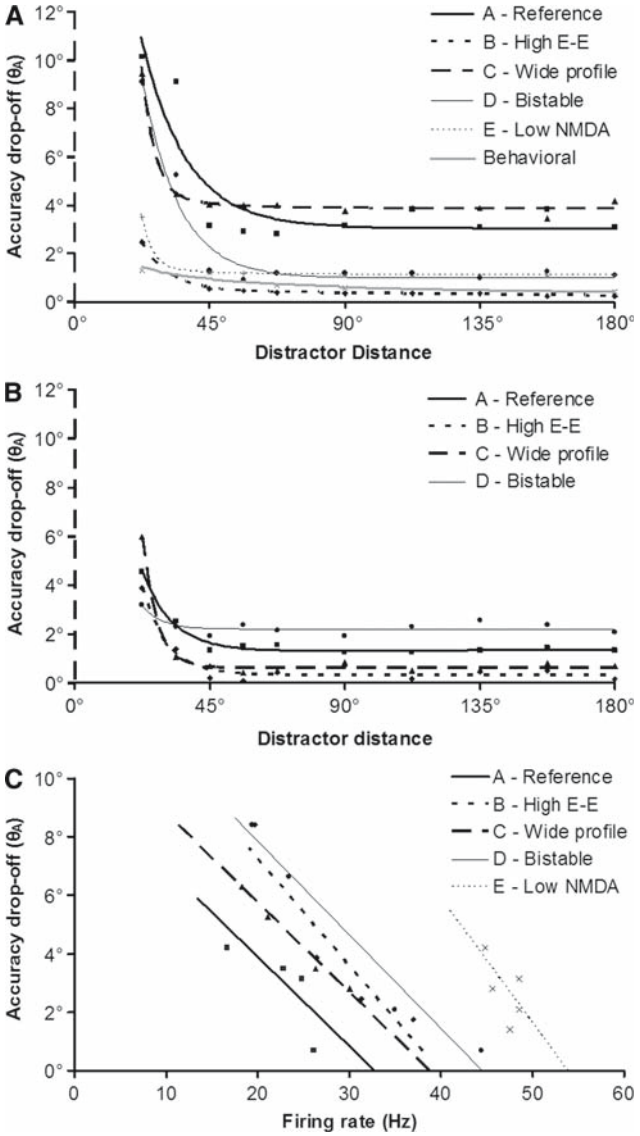

Fig. 6 Accuracy drop-off analysis for the five studied mechanisms. **a** Accuracy drop-off as a function of the distractor distance. Using the standard simulation protocol all five neural mechanisms were tested with distractors induced at ten distances, spanning from 22.5° to 180° from the initial location of the memorized cues. The series are averages of eight noisy simulations with the control baseline (no distractor) subtracted. The points are fitted with an exponential decay curve. The distractor distance effect was found to be of similar magnitude in the behavioral experiment compared to the High E-E and Low NMDA modes. **b** The firing rates of the five network modes were adjusted to similar values producing a much narrower range of accuracy drop-offs between different modes. **c** Accuracy drop-offs as a function of firing rate of the memory bump. The entire firing rate range of all modes was mapped by means of inhibitory feedback to excitatory cells (g_{IE}) variation. The standard simulation protocol with a distractor at 33.75° was used

current required to uphold the cue-induced bump attractor during the entire simulation time when a distractor is applied at 33.75°. The value chosen as reference (1.67 mS/cm^2) was the smallest value to satisfy this condition. Beyond the higher limit random persistent activity destabilizes the network. We used $g_{EE} = 1.82$ mS/cm^2 for the high excitatory connectivity simulations. The highest accuracy (lowest value) was observed in the middle of the interval ($1.73 < g_{EE} < 1.78$). Widening the connectivity footprint also seemed to improve the accuracy (Fig. 7b). σ was increased from the reference value 0.050 to 0.062, value that rendered firing rates of the bump which exceeded physiological values. Increasing the g_{CAN} value increased the depolarizing currents that entered the dendritic compartments resulting in almost monotonic accuracy improvement (Fig. 7c)

The fast excitation mediated by the AMPA receptors followed by a slower inhibition mediated by the GABA receptors promotes oscillations which destabilize the network (Wang 1999). Although the relative contribution of NMDA and AMPA receptors is still a matter of debate, physiological studies have found persistent activity to be more sensitive to NMDA receptor block than to AMPA receptor block (Dudkin et al. 1997; Shima and Tanji 1998; Aura and Riekkinen 1999). Additionally, the human prefrontal cortex is reported to have the highest NMDA receptor density of all cortical areas (Scherzer et al. 1998). While preserving the total synaptic drive we gradually decreased the NMDA-to-AMPA ratio until the persistent activity state was destabilized (Fig. 7d). If the NMDA receptor contribution is dominant the neuronal firing is asynchronous (> 75% NMDA). A decreased NMDA receptor component synchronizes the firing pattern and the sustained activity is lost (<25% NMDA). Interestingly, increasing the AMPA component improves the accuracy of the memorized cue, with the highest accuracy attained in an interval between 40 and 90% NMDA contribution to the total synaptic drive.

We further investigated how the accuracy criterion is correlated to the distractibility of the network model. Distractibility reflects the capacity to uphold the persistent activity state in the presence of distracting stimuli. Accuracy was altered by adjusting the excitatory connection strengths within physiological range ($g_{EE} = 1.57 - 1.72$ mS/cm^2). We mapped the smallest intensity of the distractor current that successfully led to the extinction of the bump attractor (Fig. 7e). We found an inverse correlation between accuracy and distractibility of a memorized cue.

4 Discussion

Our results strengthen the current hypothesis which attributes the temporary storage of the information to stimulus selective persistent neural activity—the

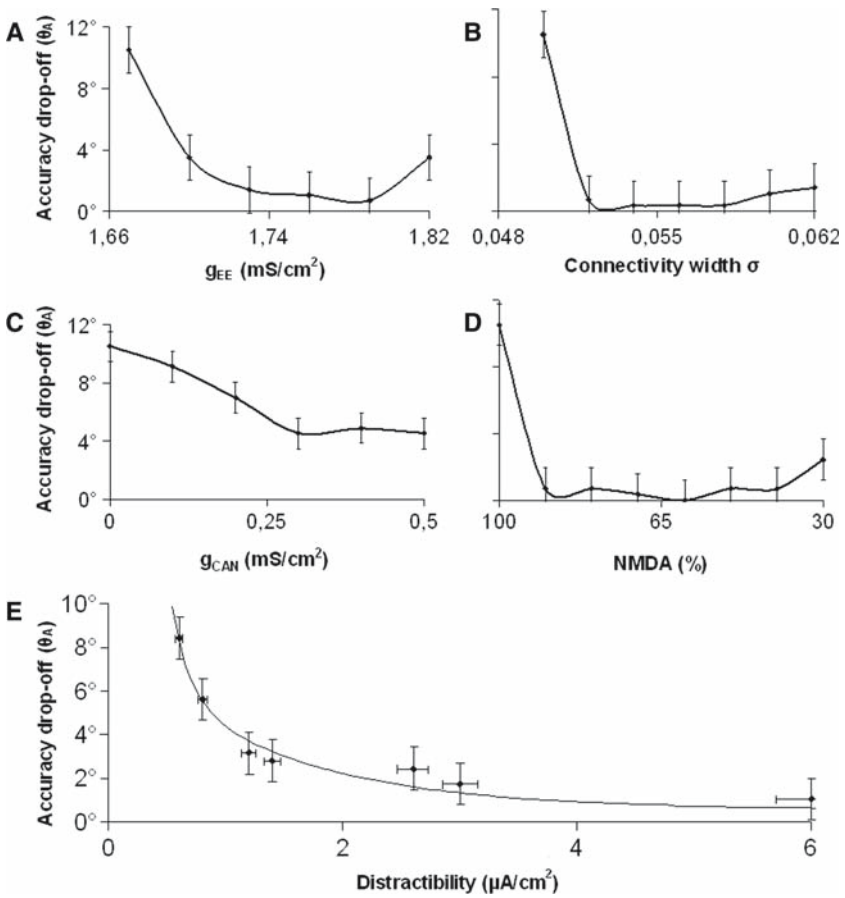

Fig. 7 Accuracy drop-off plot for mode-dependent parameter variation. Distractor present at 33.75°. **a** NMDA channel conductance between excitatory cells. **b** Width of the excitatory connectivity. **c** Dendritic CAN channel conductance. **d** Relative contribution of the NMDA receptors to the time integral of a unitary excitatory postsynaptic current EPSC (−65 mV). **e** Accuracy drop-off versus distractibility of a memorized cue. Increased cue accuracy (lower values) was correlated with higher distractor currents needed to abolish the cue-induced state of persistent activity. Every dot corresponds to a network instance with different E-E connections strengths ($g_{EE} = 1.57 - 1.72\,\mathrm{mS/cm^2}$). The distractor had the same characteristics as a cue stimulus (intensity and duration) except that it was presented 500 ms after the cue onset at 56° distance

neurophysiological correlate of working memory. Although the identity of the key cellular mechanism which underlies working memory has been controversial (Wang 2001; Miller and Cohen 2001), our work is to our knowledge the first to integrate computational modeling with behavioral experiments to evaluate different suggested neural mechanisms. Here, we have presented behavioral evidence for a strong recurrent connectivity where the firing rate during the delay plays the major role and interestingly enough, the underlying neural mechanisms generating the neuronal circuit dynamics is not crucial to explain the behavioral data. In consensus with behavioral results, we found that the sensitivity to distractors in recurrent cortical models decreases with the distractor distance to the location of the memorized cue, regardless of the neuronal mode of operation.

Secondly our study suggests that a cortical network operating in a low NMDA mode sustaining the persistent activity is not consistent with the firing rates observed in experiments. Moreover, reducing the relative amount of synaptic NMDA current, the in silico network demonstrated increased potential for synchronous oscillation between the neurons (Tegnér et al. 2002), but yet the circuit actually displays a similar distance-dependent effect of distractors as observed in the behavioral experiment. The narrow tuning curve with elevated firing rates of preferred cue neuronal population is different from previous electrophysiological findings (Funahashi et al. 1989) which could be taken as further evidence that a low NMDA mode of operation is less likely to be the case. Finally, if the recurrent excitation was supplemented with intrinsic bistability due to dendritic I_{CAN} currents, we found higher firing rates with only a slight increase in the cue accuracy. Further theoretical and experimental studies are necessary to elucidate cellular bistability of the cortical neurons.

When the excitatory synaptic input in the network was set to values in the lower regime of the physiological range, the model showed a significantly lower mnemonic accuracy compared to the behavioral results. If the connectivity profile was widened, the strength of the stronger adjacent connections could be lowered, yielding a similar bump firing rate and accuracy of the memorized cue.

Realistic distractor effects and population firing profile are found if the reverberatory synaptic input to the excitatory units is set in the higher region of the physiological range of connectivity strengths.

4.1 Accuracy of memory location

For the simulation study, we considered the difference between the accuracy drop-offs of the undisrupted cues and cues followed by distractors. This difference was compared with the corresponding behavioral values and the similarity gave the quantitative basis when evaluating the five tested neural mechanisms. We deliberately did not use the absolute accuracy drop-off values for evaluation purposes as the undisrupted "base line" accuracy drop-off depends not only on the memory decay but also on factors like the maximum value allowed for the accuracy drop-off (20° here, see Sect. 2) and the fraction of the visual field the presentation screen covers. As the network model did not account for these sources of uncertainty a comparison of the behavioral and simulated absolute accuracy drop-offs cannot be performed.

Following experimental results like (Miller et al. 1996) several previous studies (Koulakov et al. 2002; Brody et al. 2003) have stressed the necessity of robustness to distractors of cortical networks representing WM. The elevated non-selective inhibition rate of a recurrent network in persistent activity state offers resistance to intervening stimuli. This is true as long as distractor intensity is low or the distance between the bump state and distractor stimulus is sufficiently large. The persistent activity state of the network will eventually subside for high distractor amplitudes. The E to E connectivity structure of the model is the key factor understanding the distractor distance effect observed in recurrent models.

The observed instability of the memorized target location after a variable delay period has been previously studied in humans (Ploner et al. 1998) and monkeys (White et al. 1994). The loss in accuracy was attributed to both systematic errors that were similar in size for any studied delay intervals and to variable errors that increased monotonically as delay intervals were lengthened. Theoretical studies have accredited the random drift of memory to tuned inhibitory feedback on excitatory cells (Ben-Yishai et al. 1997). Our computational study suggests that the magnitude of the memory drift is correlated to the distractibility of the cue. High memory drifts imply high distractibility. The finding is however yet to be observed in behavioral experiments.

4.2 Relation to multiple-item representations

The present computational study represents one target cue along with the following distractor stimulus. This apparent difference between the computational model and the experimental design could be interpreted as weakness of the study. However, because this class of WM models can maintain multiple items (Macoveanu et al. 2006), simulating an isolated cue and distractor is highly representative even for a multiple-item model of the delayed-response task. The accuracy criterion used reflects intrinsic functional characteristics of the neuronal units and their recurrent connections, being independent of the number of represented cues. Our finding that the firing rate is the main determinant of the effect of a distractor further supports the notion that the particular neuronal mechanisms underlying a multi-item mode of operation is of less relevance here.

4.3 Experimental design considerations for distracting the human working memory

An important property of the prefrontal cortex is the extent to which it can retain information in WM in spite of distraction (Cornette et al. 2001; Sakai et al. 2002). There are numerous studies showing how working memory capacity interacts with interference. Subjects with lower working memory capacity are more prone to make erroneous saccades to irrelevant stimulus locations (Roberts et al. 1994; Kane et al. 2001). WM showed to be crucial for directing attention appropriately in selective attention tasks through the active maintenance of stimulus priorities. Consequently, a high working memory load increases the interfering effect of a distractor (de Fockert et al. 2001; Lavie et al. 2004). It thus seems as the relationship between working memory capacity and working memory load determines how much interfering effect a distractor has. Our behavioral task incorporates previous psychological and experimental knowledge of working memory capacity and distractibility. Interestingly, initially it proved difficult to distract the human subjects. We had therefore to consider the experimental design carefully. The delayed-response task was constructed to maximize the task demand thus facilitating distraction. This was achieved by using a number of cues that tapped the general visuo-spatial WM storage capacity (Todd and Marois 2004; Vogel and Machizawa 2004) and distractors which resembled the visual stimuli (Treisman and Gelade 1980). Furthermore, we considered the distracted cue from the middle of the cue sequence because of the lower retention probability of the target as predicted by the serial position effect (Thomas 1968).

4.4 Outlook and experimental predictions

The present study makes several statements and predictions. For the ensuing discussion it should be noted that a small accuracy drop-off means that a manipulation has a small effect on the accuracy; the mnemonic accuracy is therefore high under this condition.

First, mnemonic accuracy is directly proportional to the spatial distance between cue and distractor, as validated by both behavioral (Fig. 3) and computational experiments (Fig. 6a, b). A nearby distractor perturbs the cue more than a distant distractor and the behavioral response is consequently less accurate. Secondly, the computational analysis demonstrates that accuracy is also inversely proportional to distractibility (Fig. 7e). Third, it can therefore be inferred that the distance between the cue and distractor is inversely proportional to distractibility. Hence, a behaviorally weak distractor at small distance is predicted to have a similar effect on the mnemonic accuracy as behaviorally stronger or more relevant distractor at a larger distance from the encoded cue. To the best of our knowledge this has not yet been examined experimentally. Fourth, the study revealed that the firing rate and not the neural mechanism per se is directly proportional to the mnemonic accuracy (Fig. 6). Fifth, recent experimental studies (Klingberg et al. 2005) have demonstrated that the capacity of working memory, the ability to maintain several items across time can be improved through computerized working memory training. A neuronal correlate to this remarkable result has recently been identified. Imaging experiments (Olesen et al. 2004) detected that working memory training induces a selected increase of the brain activity. However, the neuronal mechanisms underlying the effects of the training are yet unclear. The present study, which demonstrates the positive correlation between the mnemonic accuracy and firing rate, suggests that the observed increase in brain activity could correlate with an increased firing rate, and therefore increased mnemonic accuracy. A recent experimental study conducted by Olesen et al. (2005) confirms a tight relation between WM capacity, delay related elevated brain activity and mnemonic accuracy. Those results in conjunction with the results of the present study predict that, after the memory training, stronger distracting stimuli are required to disrupt the mnemonic activity during a delay-period task. This is a testable suggestion. Finally, if the working memory training affects neural mechanisms in such a manner that the delay-related firing rate increases, then the present study accounts for the beneficial effects on mnemonic accuracy and distractibility.

References

Abeles M (1991) Corticonics: neural circuits of the cerebral cortex. Cambridge University Press, Cambridge

Amari S (1977) Dynamics of pattern formation in lateral-inhibition type neural fields. Biol Cybern 27:77–87

Amit DJ (1995) The Hebbian paradigm reintegrated: local reverberations as internal representations. Behav Brain Sci 18:617–626

Amit DJ, Brunel N (1997) Model of global spontaneous activity and local structured activity during delay periods in the cerebral cortex. Cereb Cortex 7:237–252

Aura J, Riekkinen P Jr (1999) Blockade of NMDA receptors located at the dorsomedial prefrontal cortex impairs spatial working memory in rats. Neuroreport 10:243–248

Baddeley A (1986) Working memory. Oxford University Press, New York

Ben-Yishai R, Bar-Or RL, Sompolinsky H (1995) Theory of orientation tuning in visual cortex. Proc Natl Acad Sci USA 92:3844–3848

Ben-Yishai R, Hansel D, Sompolinsky H (1997) Traveling waves and the processing of weakly tuned inputs in a cortical network module. J Comput Neurosci 4:57–77

Brody CD, Romo R, Kepecs A (2003) Basic mechanisms for graded persistent activity: discrete attractors, continuous attractors, and dynamic representations. Curr Opin Neurobiol 13:204–211

Brunel N (1996) Hebbian learning of context in recurrent neural networks. Neural Comput 8:1677–1710

Compte A, Brunel N, Goldman-Rakic PS, Wang XJ (2000) Synaptic mechanisms and network dynamics underlying spatial working memory in a cortical network model. Cereb Cortex 10:910–923

Compte A, Constantinidis C, Tegnér J, Raghavachari S, Chafee MV, Goldman-Rakic PS, Wang XJ (2003) Temporally irregular mnemonic persistent activity in prefrontal neurons of monkeys during a delayed response task. J Neurophysiol 90:3441–3454

Constantinidis C, Franowicz MN, Goldman-Rakic PS (2001) Coding specificity in cortical microcircuits: a multiple-electrode analysis of primate prefrontal cortex. J Neurosci 21:3646–3655

Cornette L, Dupont P, Salmon E, Orban GA (2001) The neural substrate of orientation working memory. J Cogn Neurosci 13:813–828

de Fockert JW, Rees G, Frith CD, Lavie N (2001) The role of working memory in visual selective attention. Science 291:1803–1806

Diesmann M, Gewaltig MO, Aertsen A (1999) Stable propagation of synchronous spiking in cortical neural networks. Nature 402:529–533

Dudkin KN, Kruchinin VK, Chueva IV (1997) Effect of NMDA on the activity of cortical glutaminergic structures in delayed visual differentiation in monkeys. Neurosci Behav Physiol 27:153–158

Durstewitz D, Seamans JK, Sejnowski TJ (2000) Dopamine-mediated stabilization of delay-period activity in a network model of prefrontal cortex. J Neurophysiol 83:1733–1750

Egorov AV, Hamam BN, Fransen E, Hasselmo ME, Alonso AA (2002) Graded persistent activity in entorhinal cortex neurons. Nature 420:173–178

Fransen E, Lansner A (1998) A model of cortical associative memory based on a horizontal network of connected columns. Network 9:235–264

Funahashi S, Bruce CJ, Goldman-Rakic PS (1989) Mnemonic coding of visual space in the monkey's dorsolateral prefrontal cortex. J Neurophysiol 61:331–349

Fuster JM (1973) Unit activity in prefrontal cortex during delayed-response performance: neuronal correlates of transient memory. J Neurophysiol 36:61–78

Fuster JM (1995) Memory in the cerebral cortex. MIT press, Cambrige

Fuster JM (1997) The prefrontal cortex: anatomy, physiology, and neuropsychology of the frontal lobe. Lippincott-Raven, New York

Gewaltig MO, Diesmann M, Aertsen A (2001) Propagation of cortical synfire activity: survival probability in single trials and stability in the mean. Neural Netw 14:657–673

Goldman MS, Levine JH, Major G, Tank DW, Seung HS (2003) Robust persistent neural activity in a model integrator with multiple hysteretic dendrites per neuron. Cereb Cortex 13:1185–1195

Goldman-Rakic PS (1987) Circuitry of primate prefrontal cortex and regulation of behavior by representational memory. In: Handbook of physiology. American Physiology Society, Bethesda, pp 373–417

Goldman-Rakic PS (1995) Cellular basis of working memory. Neuron 14:477–485.

Gutkin BS, Laing CR, Colby CL, Chow CC, Ermentrout GB (2001) Turning on and off with excitation: the role of spike-timing asynchrony and synchrony in sustained neural activity. J Comput Neurosci 11:121–134

Haj-Dahmane S, Andrade R (1998) Ionic mechanism of the slow afterdepolarization induced by muscarinic receptor activation in rat prefrontal cortex. J Neurophysiol 80:1197–1210

Hebb DO (1949) The organization of behaviour. Wiley, New York

Hestrin S, Sah P, Nicoll RA (1990) Mechanisms generating the time course of dual component excitatory synaptic currents recorded in hippocampal slices. Neuron 5:247–253

Hopfield JJ (1982) Neural networks and physical systems with emergent collective computational abilities. Proc Natl Acad Sci USA 79:2554–2558

Jahr CE, Stevens CF (1990) Voltage dependence of NMDA-activated macroscopic conductances predicted by single-channel kinetics. J Neurosci 10:3178–3182

Kane MJ, Bleckley MK, Conway ARA, Engle RW (2001) A controlled-attention view of working-memory capacity. J Exp Psychol Gen 130:169–183

Klingberg T, Fernell E, Olesen PJ, Johnson M, Gustafsson P, Dahlstrom K, Gillberg CG, Forssberg H, Westerberg H (2005) Computerized training of working memory in children with ADHD—a randomized, controlled trial. J Am Acad Child Adolesc Psychiatry 44:177–186

Koulakov AA, Raghavachari S, Kepecs A, Lisman JE (2002) Model for a robust neural integrator. Nat Neurosci 5:775–782

Kritzer MF, Goldman-Rakic PS (1995) Intrinsic circuit organization of the major layers and sublayers of the dorsolateral prefrontal cortex in the rhesus monkey. J Comp Neurol 359:131–143

Lavie N, Hirst A, de Fockert JW, Viding E (2004) Load theory of selective attention and cognitive control. J Exp Psychol Gen 133:339–354

Lee RH, Heckman CJ (1998) Bistability in spinal motoneurons in vivo: systematic variations in persistent inward currents. J Neurophysiol 80:583–593

Levitt JB, Lewis DA, Yoshioka T, Lund JS (1993) Topography of pyramidal neuron intrinsic connections in macaque monkey prefrontal cortex (areas 9 and 46). J Comp Neurol 338:360–376

Lisman JE, Fellous JM, Wang XJ (1998) A role for NMDA-receptor channels in working memory. Nat Neurosci 1:273–275

Loewenstein Y, Sompolinsky H (2003) Temporal integration by calcium dynamics in a model neuron. Nat Neurosci 6:961–967

Macoveanu J, Klingberg T, Tegner J (2006) A biophysical model of multiple-item working memory: a computational and neuroimaging study. Neuroscience 141:1611–1618

Markram H, Lubke J, Frotscher M, Roth A, Sakmann B (1997) Physiology and anatomy of synaptic connections between thick tufted pyramidal neurones in the developing rat neocortex. J Physiol 500(Pt 2):409–440

McCormick DA, Connors BW, Lighthall JW, Prince DA (1985) Comparative electrophysiology of pyramidal and sparsely spiny stellate neurons of the neocortex. J Neurophysiol 54: 782–806

Miller EK, Cohen JD (2001) An integrative theory of prefrontal cortex function. Annu Rev Neurosci 24:167–202

Miller EK, Erickson CA, Desimone R (1996) Neural mechanisms of visual working memory in prefrontal cortex of the macaque. J Neurosci 16:5154–5167

Mountcastle VB (1997) The columnar organization of the neocortex. Brain 120(Pt 4):701–722

Norman DA (1970) Models of human memory. Academic, New York

Olesen PJ, Westerberg H, Klingberg T (2004) Increased prefrontal and parietal activity after training of working memory. Nat Neurosci 7:75–79

Olesen PJ, Macoveanu J, Klingberg T (2005) Childhood development of brain activity related to working memory and distractor processing (unpublished)

Ploner CJ, Gaymard B, Rivaud S, Agid Y, Pierrot-Deseilligny C (1998) Temporal limits of spatial working memory in humans. Eur J Neurosci 10:794–797

Roberts RJ, Hager LD, Heron C (1994) Prefrontal cognitive processes working memory and inhibition in the antisaccade task. J Exp Psychol Gen 123:374–393

Sakai K, Rowe JB, Passingham RE (2002) Active maintenance in prefrontal area 46 creates distractor-resistant memory. Nat Neurosci 5:479–484

Salin PA, Prince DA (1996) Electrophysiological mapping of GABAA receptor-mediated inhibition in adult rat somatosensory cortex. J Neurophysiol 75:1589–1600

Sandberg A, Tegnér J, Lansner A (2003) A working memory model based on fast Hebbian learning. Network 14:789–802

Scherzer CR, Landwehrmeyer GB, Kerner JA, Counihan TJ, Kosinski CM, Standaert DG, Daggett LP, Velicelebi G, Penney JB, Young AB (1998) Expression of N-methyl-D-aspartate receptor subunit mRNAs in the human brain: hippocampus and cortex. J Comp Neurol 390:75–90

Schiller J, Schiller Y (2001) NMDA receptor-mediated dendritic spikes and coincident signal amplification. Curr Opin Neurobiol 11:343–348

Seung HS (1996) How the brain keeps the eyes still. Proc Natl Acad Sci USA 93:13339–13344

Seung HS, Lee DD, Reis BY, Tank DW (2000) Stability of the memory of eye position in a recurrent network of conductance-based model neurons. Neuron 26:259–271

Shima K, Tanji J (1998) Involvement of NMDA and non-NMDA receptors in the neuronal responses of the primary motor cortex to input from the supplementary motor area and somatosensory cortex: studies of task-performing monkeys. Jpn J Physiol 48:275–290

Singer W (1993) Synchronization of cortical activity and its putative role in information processing and learning. Annu Rev Physiol 55:349–374

Spruston N, Jonas P, Sakmann B (1995) Dendritic glutamate receptor channels in rat hippocampal CA3 and CA1 pyramidal neurons. J Physiol 482(Pt 2):325–352

Tegnér J, Compte A, Wang XJ (2002) The dynamical stability of reverberatory neural circuits. Biol Cybern 87:471–481

Thomas HB (1968) An information-theoretic model for the serial position effect. Psychol Rev 75:409–420

Todd JJ, Marois R (2004) Capacity limit of visual short-term memory in human posterior parietal cortex. Nature 428:751–754

Treisman AM, Gelade G (1980) A feature-integration theory of attention. Cognit Psychol 12:97–136

Vogel EK, Machizawa MG (2004) Neural activity predicts individual differences in visual working memory capacity. Nature 428:748–751

Wang XJ (1999) Synaptic basis of cortical persistent activity: the importance of NMDA receptors to working memory. J Neurosci 19:9587–9603

Wang XJ (2001) Synaptic reverberation underlying mnemonic persistent activity. Trends Neurosci 24:455–463

Wang XJ, Tegnér J, Constantinidis C, Goldman-Rakic PS (2004) Division of labor among distinct subtypes of inhibitory neurons in a cortical microcircuit of working memory. Proc Natl Acad Sci USA 101:1368–1373

White JM, Sparks DL, Stanford TR (1994) Saccades to remembered target locations: an analysis of systematic and variable errors. Vis Res 34:79–92

Xiang Z, Huguenard JR, Prince DA (2002) Synaptic inhibition of pyramidal cells evoked by different interneuronal subtypes in layer v of rat visual cortex. J Neurophysiol 88:740–750